sections are caused by overlapping resonances where the wave functions describing the temporarily captured electron resemble the virtual orbitals. The contributions of individual orbitals to the vibrational cross section will be strongly affected by their lifetimes, controlled by the height of the centrifugal barrier and thus by the symmetry and nodal properties. (In particular, the A_1' orbitals, such as the second LUMO, will couple strongly to the s-wave.) The situation is further complicated by possible mixing of resonances with the same symmetry and possible vibronic coupling of resonances of different symmetries. Finally, one may be tempted to interpret some finer details of the excitation functions in Figure 3 using the virtual orbitals. The fact that the onset of the broad band lies lower in the ν_1 excitation curves than in the $2\nu_3$ excitation curve could be explained by the second LUMO a_1', which is antibonding in C-H but not in C-C, and lies well below the other σ^* orbitals (Figure 9). We feel, however, that such assignments remain speculative without better understanding of the relation between higher-lying virtual orbitals and shape resonances.

Visual inspection of the shapes of the σ^* orbitals indicates that a wide range of partial waves will be associated with the different resonances. It is not unreasonable to expect that the resulting angular distribution is almost isotropic.

V. Conclusion

The extraordinary structure of [1.1.1]propellane is reflected in its electronic structure, which is strikingly different from that of a saturated hydrocarbon. The first vertical attachment energy is nearly identical with that of ethene. Similarly, the first triplet band is at nearly the same energy, and even has the same appearance, as the first triplet band in ethene. The shapes of the triplet band, the negative ion band, and the degree and selectivity of resonant vibrational excitation are well in line with a LUMO which is antibonding along the bridging bond. On the other hand, the band which appears to correspond to the dipole-allowed HOMO → LUMO singlet transition is remarkably narrow. Additional bands in vibrational cross section in the 3-15-eV region indicate short-lived shape resonances which we associate with higher-lying σ^* orbitals. These orbitals play an important role in hyperconjugation, and we plan to continue to study them with the same methodology in other, less "exotic" hydrocarbons.

Acknowledgment. We express our sincere appreciation to Professor E. Haselbach for his continuing support and encouragement in the present work. The construction of the spectrometers represents a major effort in terms of development and fabrication of the mechanical and electronical components. These tasks have been accomplished by E. Brosi of the mechanical laboratory and P.-H. Chassot of the electronical laboratory. The present work would not be possible without their exceptional enthusiasm and ingenuity in finding solutions for all the innumerous problems encountered in the course of the construction. We thank T. Bally and P. Jungwirth for help with the Gaussian program and K. Jordan for kind comments on the manuscript. Financial support by the Deutsche Forschungsgemeinschaft is gratefully acknowledged. This work is part of Project 20-28842.90 of the Schweizerischer Nationalfonds zur Förderung der wissenschaftlichen Forschung.

Models for Polysilane High Polymers. 2. Photophysics of Linear Permethylhexasilane: A Low-Lying Franck-Condon Forbidden Excited Singlet State

Ya-Ping Sun and Josef Michl*[,1]

Contribution from the Department of Chemistry and Biochemistry, University of Colorado, Boulder, Colorado 80309-0215. *Received April 9, 1992*

Abstract: The UV absorption properties of Si_6Me_{14} are those expected from an extrapolation from longer chains, but its fluorescence is not. The observations are best accommodated by postulating that the emitting state of Si_6Me_{14} is distinct from the $\sigma\sigma^*$ state that dominates its absorption, in contrast to the situation in $Si_{10}Me_{22}$ and longer oligosilanes. Tentative assignments are considered for the emitting state. The fluorescence quantum yield of Si_6Me_{14} is strongly temperature dependent, suggesting the existence of a thermally activated radiationless decay channel (E_a = 2.1 kcal/mol, $A = 2 \times 10^{12}$ s^{-1}).

Introduction

Polysilanes, a relatively new class of σ-conjugated polymers, have attracted considerable interest.[2-6] Photophysical and photochemical studies have been focusing on their electronic structure, conformation, and photochemical degradation.[7-11]

The quite unique photophysical and photochemical properties of room-temperature polysilane solutions have been interpreted in terms of the segment distribution model.[7,8,10] In this model it is assumed that the polysilane chain consists of a series of approximately planar all-trans segments separated by one or more approximately gauche twists of the backbone and acting as nearly localized chromophores of different length and energy. The inhomogeneous distribution of the chromophoric segments, their spectroscopic properties, and their energy transfer processes are then assumed to dictate the optical properties of polysilane high

(1) The bulk of this work was performed while the authors were still at the Center for Structure and Reactivity, Department of Chemistry and Biochemistry, University of Texas at Austin, Austin, Texas 78712.

(2) Michl, J.; Sun, Y.-P. In *Radiation Effects on Polymeric Materials*; Reichmanis, E., O'Donnell, J. H., Frank, C. W., Eds.; ACS Symposium Series; American Chemical Society: Washington, DC, in press.

(3) Michl, J. *Synth. Met.*, in press.

(4) Miller, R. D.; Michl, J. *Chem. Rev.* **1989**, *89*, 1359.

(5) Zeigler, J. M. *Synth. Met.* **1989**, *28*, C581; *Mol. Cryst. Liq. Cryst.* **1990**, *190*, 265.

(6) West, R. *J. Organomet. Chem.* **1986**, *300*, 327.

(7) (a) Michl, J.; Downing, J. W.; Karatsu, T.; Klingensmith, K. A.; Wallraff, G. M.; Miller, R. D. In *Inorganic and Organometallic Polymers*; Zeldin, M., Wynne, K., Allcock, J., Eds.; ACS Symposium Series 360; American Chemical Society: Washington, DC, 1988, Chapter 5. (b) Klingensmith, K. A.; Downing, J. W.; Miller, R. D.; Michl, J. *J. Am. Chem. Soc.* **1986**, *108*, 7438.

(8) Harrah, L. A.; Zeigler, J. M. *Macromolecules* **1987**, *20*, 601.

(9) (a) Thorne, J. R. G.; Williams, S. A.; Hochstrasser, R. M.; Fagan, P. J. *Chem. Phys.* **1991**, *157*, 401. (b) Thorne, J. R. G.; Repinec, S. T.; Abrash, S. A.; Zeigler, J. M.; Hochstrasser, R. M. *Chem. Phys.* **1990**, *146*, 315.

(10) Sun, Y.-P.; Miller, R. D.; Sooriyakumaran, R.; Michl, J. *J. Inorg. Orgnomet. Polym.* **1991**, *1*, 3.

(11) (a) Michl, J.; Downing, J. W.; Karatsu, T.; McKinley, A. J.; Poggi, G.; Wallraff, G. M.; Sooriyakumaran, R.; Miller, R. D. *Pure Appl. Chem.* **1988**, *60*, 959. (b) Miller, R. D.; Rabolt, J. F.; Sooriyakumaran, R.; Fleming, W.; Fickes, G. N.; Farmer, B. L.; Kuzmany, H. In *Inorganic and Organometallic Polymers*; Zeldin, M., Wynne, K., Allcock, J., Eds.; ACS Symposium Series 360; American Chemical Society: Washington, DC, 1988, Chapter 4.

0002-7863/92/1514-8186$03.00/0

polymers. It is therefore of interest to investigate relatively short oligosilane chains as models for the understanding of excited states and conformations of polysilanes in general. The near-UV absorption bands of these materials were reported quite some time ago,[12] but little if any attention has been paid to their emission.

It has been noted recently that the photophysical properties of permethylated silane oligomers rapidly approach those of the polymers as the silicon chain length is increased. Permethylhexadecasilane ($Si_{16}Me_{34}$) already is very similar to poly(dialkylsilane)s in nearly every respect, especially in room-temperature solution.[13] The absorption and fluorescence of permethyldecasilane ($Si_{10}Me_{22}$) are more clearly different.[2,14]

We now report that the photophysical properties of an even shorter oligosilane, permethylhexasilane (Si_6Me_{14}), are very different and attribute this to a change in the nature of the lowest excited singlet state. A state crossing has been postulated previously in order to account for the photophysics of the high polymers.[10] It was also predicted to occur by ab initio calculations,[15,16] albeit at shorter chain lengths.

Experimental Section

Materials. 3-Methylpentane (Phillips Pure Grade or Aldrich 99+%) and hexane (Baker Photrex) were purified by the procedures described in ref 10. 9,10-Diphenylanthracene (Aldrich Gold Label, 99+%) was used as a fluorescence standard.

1,6-Dichlorododecamethylhexasilane. Dodecamethylcyclohexasilane[17] was chlorinated as reported[18,19] except that 3 equiv of chlorine in carbon tetrachloride was used. The yield is higher with PCl_5, giving 80% product after distillation: bp 150–155 °C (0.2 Torr); ^{1}H NMR δ 0.24 (s, 12 H), 0.25 (s, 12 H), 0.52 (s, 12 H); ^{13}C NMR δ −5.89, −4.54, 3.36; EIMS *m/z* 403 (8), 383 (M − Cl − 15, 5), 325 (10), 267 (100), 209 (68), 174 (40), 159 (22), 131 (50), 73 (71), 57 (50).

Permethylhexasilane.[20] A solution of 1,6-dichlorododecamethylsilane (180 mg, 0.44 mmol) in hexane (2 mL) was treated with an excess of methylmagnesium bromide (180 mg) in diethyl ether. The solution was refluxed for 24 h, then treated with dilute hydrochloric acid, extracted with hexanes, dried with magnesium sulfate, and concentrated. The sample was separated by preparative gas–liquid chromatography, yielding crystalline permethylhexasilane (106 mg, 65% yield): mp 29 °C (lit[20] mp 28–29 °C); ^{1}H NMR δ 0.9 (s, 18 H), 0.13 (s, 12 H), 0.17 (s, 12 H); ^{13}C NMR δ −5.67, −4.35, −1.24; EIMS *m/z* 379 (M + 1, 2), 378 (M, 5), 305 (1), 247 (5), 231 (4), 189 (13), 173 (27), 157 (7), 131 (15), 116 (10), 73 (100).

Measurements. Melting points were determined using a Boetius PHMK05 apparatus with a microscope attachment at a warm-up rate of 4 °C/min or in a sealed capillary. NMR spectra were measured in $CDCl_3$ on a 360-MHz Nicolet NT-360 instrument. Chemical ionization (CI) and electron impact (EI) mass spectra were obtained on a Bell & Howell 21-491 and a VG ZAB-2E mass spectrometers. Absorption spectra were recorded on a Cary 2300 absorption spectrophotometer. Fluorescence spectra were measured on an SLM Aminco SPF-500C emission spectrophotometer equipped with a 300-W Xe lamp using a right-angle geometry. Polarized fluorescence spectra were obtained on a home-built spectrofluorimeter.[7a] Spectra in room-temperature solution were obtained using a 1-cm square cell, and spectra in 77 K glass were obtained in a quartz dewar with three Suprasil windows filled with liquid nitrogen. Because of the technical difficulty of matching the experimental condition of the standard with that of the sample in an optical dewar, the fluorescence quantum yield of Si_6Me_{14} in 3-methylpentane glass at 77 K was determined using a low concentration of diphenylanthracene (optical density 0.1 at 38 500 cm^{-1}, Φ_F = 1.0[21]) as an internal standard. The absorption spectrum of the mixture was fitted very well as a sum of the spectra of diphenylanthracene and Si_6Me_{14}. Successive dilutions of the mixture, up to 100-fold, had no effect on the ratio of the integrated fluoresence intensities of Si_6Me_{14} and the standard.

Fluorescence lifetimes were measured by using a time-correlated single photon counting spectrometer in the Center for Fast Kinetics Research at the University of Texas at Austin. Quadrupled (266-nm) light from a Coherent Antares Nd:YAG laser mode-locked at ca. 86 MHz was used for excitation. The same laser beam was split to synchronously pump a cavity-dumped Rhodamine-B dye laser to drive the detection system. Fluorescence decays were monitored by a Hamamatsu R1564U microchannel plate photomultiplier tube at right angles to the excitation beam. A monochromator was used for the selection of monitored emission frequency.

The temperature dependence of the fluorescence quantum yield and lifetime was measured in the optical dewar using nitrogen gas as coolant. The temperature was measured to within a few degrees by a thermocouple placed immediately next to the sample cell.

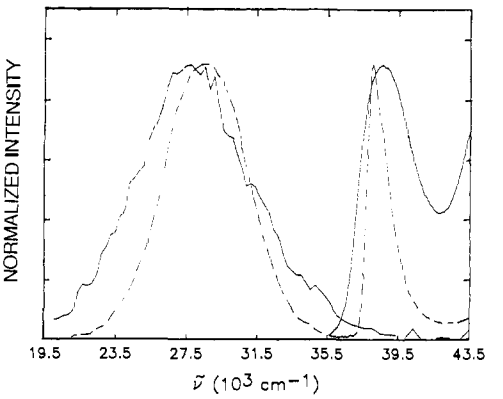

Figure 1. Absorption and fluorescence spectra of Si_6Me_{14} in room-temperature hexane solution (—), $\tilde{\nu}^{exc}$ = 38 500 cm^{-1} and in 77 K 3-methylpentane glass (---), $\tilde{\nu}^{exc}$ = 37 900 cm^{-1}.

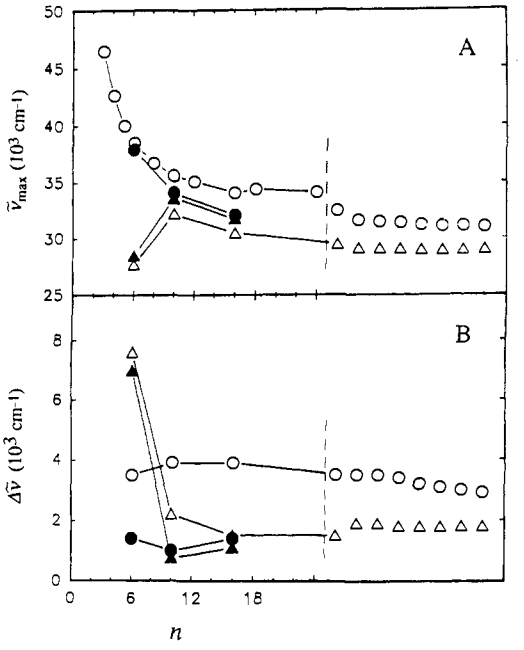

Figure 2. Absorption and fluorescence spectral maxima $\tilde{\nu}_{max}$ (A) and band widths at half maximum $\Delta\tilde{\nu}$ (B) of Si_nMe_{2n+2} plotted against the number of silicon atoms *n*. The circles are for absorption and triangles for fluorescence. The open symbols are for room-temperature solution and filled symbols for 77 K glass. Data for the oligomers other than Si_6Me_{14} are from refs 13, 14, and 22. Data for some high molecular weight poly(dialkylsilane)s[10,13] are also plotted at the right side of the dashed line for comparison, from left to right: $[CH_3(C_3H_7)Si]_x$, $[(C_4H_9)_2Si]_x$, $[(C_6H_{11})_2Si]_x$, $[(C_7H_{15})_2Si]_x$, $[(C_8H_{17})_2Si]_x$, $[(C_{10}H_{21})_2Si]_x$, $[(C_{12}H_{25})_2Si]_x$, and $[(C_{14}H_{29})_2Si]_x$.

(12) (a) Gilman, H.; Atwell, W. H.; Schwebke, G. L. *J. Organomet. Chem.* **1964**, *2*, 369. (b) Sakurai, H.; Kumada, M. *Bull. Chem. Soc. Jpn.* **1964**, *37*, 1894.

(13) Sun, Y.-P.; Hamada, Y.; Huang, L. M.; Maxka, J.; Hsiao, J.-S.; West, R.; Michl, J. *J. Am. Chem. Soc.* **1992**, *114*, 6301.

(14) Sun, Y.-P.; Veas, C.; Hamada, Y.; Huang, L. M.; West, R.; Michl, J. Unpublished results.

(15) Michl, J.; Balaji, V. In *Computational Advances in Organic Chemistry*; Ögretir, C., Csizmadia, I. G., Eds., NATO Advanced Study Institute Series C; Kluwer Academic Publishers: Dordrecht, Holland, 1991, p 323.

(16) Balaji, V.; Michl, J. *Polyhedron* **1991**, *10*, 1265.

(17) Carberry, E.; West, R. *J. Am. Chem. Soc.* **1969**, *91*, 5440; *J. Organomet. Chem.* **1966**, *6*, 582.

(18) Wojnowski, W.; Hurt, C. J.; West, R. *J. Organomet. Chem.* **1977**, *124*, 271.

(19) Gilman, H.; Inoue, S. *J. Organomet. Chem.* **1968**, *15*, 237.

(20) Kumada, M.; Ishikawa, M. *J. Organomet. Chem.* **1963**, *1*, 153.

(21) Parker, C. A. *Photoluminescence of Solutions*; Elsevier: Amsterdam, 1968.

(22) (a) Drenth, W.; Noltes, J. G.; Bulten, E. J.; Creemers, H. M. J. C. *J. Organomet. Chem.* **1969**, *17*, 173. (b) Boberski, W. G.; Allred, A. L. *J. Organomet. Chem.* **1975**, *88*, 65.

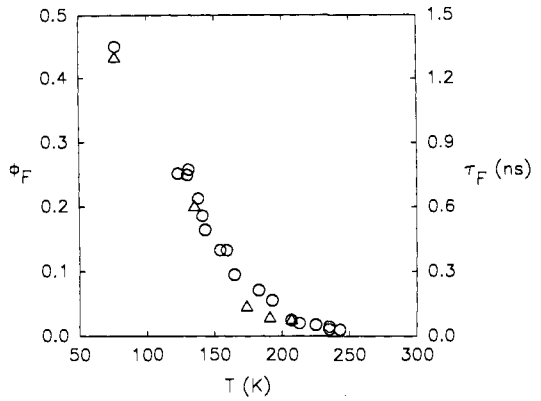

Figure 3. The fluorescence quantum yield (○) and lifetime (△) of Si_6Me_{14} in 3-methylpentane as a function of temperature.

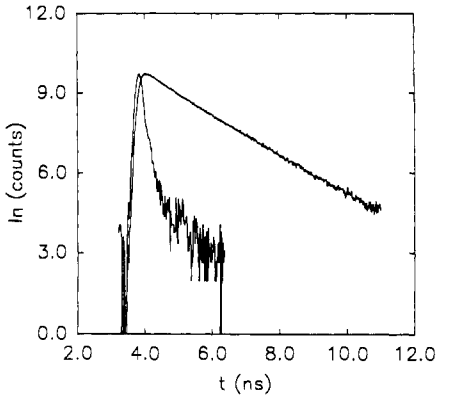

Figure 4. The fluorescence decay of Si_6Me_{14} in 77 K 3-methylpentane glass, $\tilde{\nu}^{exc}$ = 37 600 cm^{-1} and $\tilde{\nu}^{em}$ = 28 600 cm^{-1} (τ_F = 1.3 ns). The instrumental response function and the decay curve are plotted using a log scale.

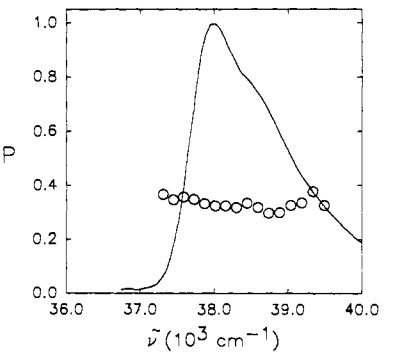

Figure 5. The degree of fluorescence polarization as a function of $\tilde{\nu}^{exc}$ for Si_6Me_{14} in 77 K 3-methylpentane glass. The monitored emission energy is 28 600 cm^{-1}.

Results

The absorption and emission spectra of Si_6Me_{14} are independent of the sample concentration (2×10^{-5} to 2×10^{-7} M), and the low-temperature spectra are independent of the rate of cooling. This behavior is very different from that of $Si_{16}Me_{34}$.[13]

Like polysilane high polymers[10] and the longer chain oligomers $Si_{10}Me_{22}$[2,14] and $Si_{16}Me_{34}$,[13] a room-temperature hexane solution of Si_6Me_{14} exhibits a strong absorption band in the near-UV region (Figure 1). The absorption spectrum consists of a nearly Gaussian first band, $\tilde{\nu}^{abs}_{max}$ = 38 500 cm^{-1} (ϵ_{max} = 24 800), blue-shifted relative to those of the longer linear oligomers.[13] A plot of the energy of the absorption maximum against the number of silicon atoms in the chain is shown in Figure 2A. The bandwidth is compatible with those of $Si_{10}Me_{22}$, $Si_{16}Me_{34}$, and the polymers (Figure 2B).

Si_6Me_{14} is only very weakly fluorescent in room-temperature solution. The emission consists of a very broad band ($\Delta\tilde{\nu}$ = 7600 cm^{-1}) with a maximum red-shifted by about 10 000 cm^{-1} from the absorption maximum. Since the emission is very weak, the recorded spectrum is quite noisy (Figure 1). Plots of fluorescence energy and bandwidth against the number of silicon atoms in the chain are also shown in Figure 2A and B, respectively.

In a 3-methylpentane glass at 77 K the absorption band becomes much narrower ($\Delta\tilde{\nu}$ = 1400 cm^{-1}). The absorption at the low-energy side does not change much, but the absorption at the high-energy side is significantly reduced. This results in a red shift of 640 cm^{-1}. The red shift is somewhat smaller than that in the longer chain oligomers: 1500 cm^{-1} in $Si_{10}Me_{22}$ and 2000 cm^{-1} in $Si_{16}Me_{34}$.

In contrast to the absorption, the fluorescence spectrum of Si_6Me_{14} remains very broad upon cooling ($\Delta\tilde{\nu}$ = 5350 cm^{-1}) and continues to show a large Stokes shift (9400 cm^{-1}). It is independent of excitation energy. The position of the fluorescence maximum does not shift much upon cooling.

The fluorescence quantum yield Φ_F of Si_6Me_{14} in room-temperature solution is estimated to be less than 10^{-4}. Upon cooling, it increases continuously (Figure 3). The value of Φ_F in 77 K glass is 0.45 ± 0.05, an increase of at least 3 orders of magnitude from the value in room-temperature solution. The fluorescence quantum yield in a 77 K glass is independent of excitation energy, and the fluorescence excitation spectrum essentially coincides with the absorption spectrum.

The fluorescence decay in 77 K glass was fitted very well by a single exponential function (Figure 4), yielding a lifetime of 1.3 ± 0.1 ns. Also at the four other temperatures at which the fluorescence decays were measured, they were deconvoluted from instrumental response with single exponential functions. The lifetime value increases with decreasing temperature in the same way as the fluorescence quantum yield (Figure 3).

The degree of fluorescence polarization in 77 K glass is 0.35 ± 0.03. It is independent of the excitation energy (Figure 5) and the monitored emission energy.

Discussion

The Absorbing and Emitting States. As shown in Figures 1 and 2, both in a room-temperature solution and in a 77 K glass, the absorption spectra of Si_6Me_{14} extrapolate smoothly from those of the higher oligomers and the polymers, suggesting that the transitions observed in these linear permethylated silicon chain molecules are all of the same character. By now, they have been well established as due to a $\sigma\sigma^*$ (HOMO–LUMO) excitation.[4] The blue shift in Si_6Me_{14} can be attributed to its short chain length, the same as the blue shift from $Si_{16}Me_{34}$[13] to $Si_{10}Me_{22}$.[14] The thermochromic shift in Si_6Me_{14} is somewhat smaller than that in $Si_{10}Me_{22}$, presumably because the room-temperature solution of the latter contains a wider variety of conformers differing more in their absorption properties (Figure 1).

Unlike absorption, the fluorescence of Si_6Me_{14} does not meet expectations based on an extrapolation from the longer-chain oligomers at all. From Figure 2 it can be seen that the fluorescence bandwidth, the Stokes shift, and the temperature effect for Si_6Me_{14} are completely different from those found with its longer-chain homologues. Since room-temperature conformational changes are surely continuous with decreasing silicon chain length, they do not provide an explanation for the abruptly different fluorescence properties of Si_6Me_{14}.

An immediate suspicion is that the fluorescence of Si_6Me_{14} is from a less strongly allowed and Franck–Condon forbidden (i.e., geometrically distorted) excited state lying somewhat lower in energy than the strongly allowed $\sigma\sigma^*$ state that dominates the absorption spectrum, and that the transition from the ground state to the emitting state is covered up and hard to see in ordinary absorption spectra. If this is correct, the reversal of the two excited states must occur somewhere between Si_6Me_{14} and $Si_{10}Me_{22}$. A state order change in very short oligosilane chromophores had been postulated previously to explain the fluorescence properties of poly(di-*n*-alkylsilane)s in room-temperature solutions.[10]

In search of support for this proposal, we looked for a discrepancy between the experimentally determined fluorescence radiative rate constant, $k_F = \Phi_F/\tau_F$, and the calculated one, k_F^{calcd},

obtained from the integrated intensity of the first absorption band:[23,24]

$$k_F^{calcd} = 2.88 \times 10^{-9} n^2 (\bar{\nu}_{max}^{abs})^2 \int \epsilon \, d\bar{\nu} \quad (1)$$

From the absorption spectrum of Si_6Me_{14} in 77 K 3-methylpentane glass, a k_F^{calcd} value of 1×10^9 s^{-1} is obtained. This is almost triple the experimental k_F value of 3.5×10^8 s^{-1} obtained from Φ_F and τ_F values in 77 K glass, suggesting that the emitting state of Si_6Me_{14} is indeed a less strongly allowed excited state and not the one responsible for the strong absorption band. Note that for the longer oligosilanes,[13,14] the k_F^{calcd} value agrees within 20% with k_F.

It is possible that the intrinsic intensities of the two states differ by a factor much larger than 3 and that much of the intensity of the emission of Si_6Me_{14} is borrowed from the strong $\sigma\sigma^*$ transition. Since the transition moment direction would be borrowed along with the intensity, the observed positive polarization of the fluorescence excited in the $\sigma\sigma^*$ region is not surprising, but also contains no information about the intrinsic symmetry of the emitting electronic state. However, since vibronic intensity borrowing should contribute to the absorption spectrum as well, although perhaps less strongly, it is peculiar that no indication of the presence of a second transition is seen in the low-temperature absorption spectrum of Figure 1. We shall return to this point below.

The presently available information does not permit an unambiguous assignment of the nature of the proposed less strongly allowed excited state. There are three types of calculated[15,16] low-energy excited singlet states that represent reasonable candidates. (i) One class is of the $\sigma\sigma^*$ type. For most relevant Si–Si–Si valence angles, the lowest-energy state of this kind is dominated by a single configuration (HOMO–LUMO), although others contribute as well. In a planar all-trans conformation, this transition is very intense and is polarized along the direction of the silicon chain. It is conceivable that one of the other $\sigma\sigma^*$ states lies below the HOMO–LUMO state. (ii) A second class of transition is of the $\sigma\pi^*$ type. At planar all-trans geometries, transitions into these states are polarized perpendicular to the plane of the silicon atoms and should be more weakly allowed. (iii) A third class is of the Rydberg type. For the shortest oligosilanes, the energy of these states is computed to be the lowest,[15] but it does not drop as fast with increasing chain length as is the case for the other two classes, particularly the $\sigma\sigma^*$ states. We consider the Rydberg assignment the least likely.

(i) A $\sigma\sigma^*$ assignment other than HOMO–LUMO looks unlikely at first sight. First of all, the polarization of transitions into the only very weakly one-photon allowed states containing the SHOMO–LUMO and HOMO–SLUMO configurations should be along the short in-plane axis, and if one of these were the emitting state, the intrinsic polarization of the fluorescence should be negative. However, the intensity of the observed emission is probably largely borrowed from the intense HOMO–LUMO transition, along with the polarization, so that the observed polarization alone does not exclude such an assignment.

Second, at ground-state equilibrium geometries, the second HOMO (SHOMO) to LUMO, HOMO to second LUMO (SLUMO), and $HOMO^2$ to $LUMO^2$ excited configurations are calculated[16] to lie much higher in energy than the HOMO–LUMO excited configuration and to interact little with each other or with other configurations. Indeed, on the basis of these ab initio calculations it has been proposed[16] that the state observed[25] in polysilanes by two-photon absorption about 1 eV above the lowest $\sigma\sigma^*$ state is described predominantly by the SHOMO–LUMO configuration, and that the two-photon state observed[9] at about twice the energy of the $\sigma\sigma^*$ HOMO–LUMO state is described predominantly by the $HOMO^2$–$LUMO^2$ configuration. In the shorter chains, these energy differences should be larger still. Other $\sigma\sigma^*$ configurations are even less likely to contribute significantly to low-lying states.

However, since the geometry of the emitting state is clearly strongly distorted away from the equilibrium geometry of the ground state, it is necessary to consider the possibility that a suitable distortion might reach a minimum in the first excited singlet potential energy surface at a geometry quite distinct from the equilibrium geometry of the ground state and that at this distorted geometry, the excited singlet state would still be of $\sigma\sigma^*$ character, but less strongly allowed. We consider this the most likely explanation, as it most readily accounts for the absence of a second band in absorption, given a factor of only 3 in the expected oscillator strengths.

A likely distortion in all $\sigma\sigma^*$ states is an increase in the Si–Si bond length. For instance, a calculation[15] for Si_3H_8 suggests a total Si–Si bond dissociation in the triplet, and a significant bond length extension in the singlet (the difference between the two is related to the different dissociation limits[26]). The Franck–Condon allowed shape of the allowed lowest singlet $\sigma\sigma^*$ transition in the longer oligosilanes leaves no doubt that the excitation is delocalized and that the bond stretching is minimal and distributed over many Si–Si bonds. The absorption spectrum of Si_6Me_{14} suggests strongly that such a vertical local feature is present in its S_1 surface as well. In addition, however, there might be an even lower minimum at a low-symmetry geometry with one Si–Si distance greatly extended and the others normal. At this distorted geometry, the HOMO and LUMO would both be localized on the stretched bond. The excited singlet wave function, somewhat similar to that of the B state of the H_2 molecule but polarized toward one of the bond termini, would be describable approximately either as an Si^+Si^- ion pair at the stretched bond in the valence-bond language, or as a localized HOMO–LUMO excitation in the molecular orbital language.[26] This dipolar excited state would then be responsible for the emission, with a transition moment oriented roughly along the stretched Si–Si bond, at about 30–35° to the long axis of the chain, so that the expected polarization degree would be about 0.3, as observed. The emissive minimum might be accessible from the vertical geometry over a small barrier, or possibly even without a barrier.

This assignment of the emissive state of Si_6Me_{14} would be similar to the assignment proposed very recently[9a] for the emissive state of partly phenylated and partly methylated nine-silicon chain units imbedded in a polymer chain (self-trapped exciton in solid-state physicist's language).

(ii) A $\sigma\pi^*$ assignment of the proposed new state is the other serious contender. Recent ab initio calculations on the parent oligosilanes suggested[16] that the relative energies of the HOMO–LUMO $\sigma\sigma^*$ state and the $\sigma\pi^*$ state cross as the silicon chain length decreases, since the $\sigma\sigma^*$ state energy increases faster than the $\sigma\pi^*$ state energy. In long chain oligosilanes the $\sigma\sigma^*$ state is calculated to be the lowest excited state, and in short chain oligosilanes the $\sigma\pi^*$ state becomes the lowest. Depending on the calculation employed, tetrasilane or trisilane was the first chain with the $\sigma\sigma^*$ state as the lowest. However, the effect of permethylation and possible geometrical distortions might shift the cross-over point to longer chains. Also, the calculations were not quantitatively accurate and may have overestimated the relative energy of the $\sigma\pi^*$ state.

This state order change is reminiscent of the state order change with conjugated carbon chain length observed in polyenes and diphenylpolyenes, where the relative energies of the strongly allowed $1B_u$ state and the forbidden $2A_g$ state depend on the polyene chain length.[27,28] The $2A_g$ state of polyenes and diphenylpolyenes

(23) Berlman, I. B. *Mol. Cryst.* **1968**, *4*, 157.
(24) (a) Strickler, S. J.; Berg, R. A. *J. Chem. Phys.* **1962**, *37*, 814. (b) Birks, J. B.; Dyson, D. J. *Proc. R. Soc. London, A* **1963**, *275*, 135.
(25) Thorne, J. R. G.; Ohsako, Y.; Zeigler, J. M.; Hochstrasser, R. M. *Chem. Phys. Lett.* **1989**, *162*, 455. Schellenberg, F. M.; Byer, R. L.; Miller, R. D. *Chem. Phys. Lett.* **1990**, *166*, 331.
(26) Michl, J.; Bonačič-Koutecký, V. *Electronic Aspects of Organic Photochemistry*; Wiley: New York, 1990, Chapter 4.
(27) Hudson, B. S.; Kohler, B. E. *J. Chem. Phys.* **1973**, *59*, 4984.
(28) (a) Hudson, B. S.; Kohler, B. E.; Schulten, K. In *Excited States*; Lim, E. C., Ed.; Academic Press: New York, 1982; Vol. 6, p 1. (b) Saltiel, J.; Sun, Y.-P. In *Photochromism, Molecules and Systems*; Dürr, H., Bouas-Laurent, H., Eds.; Elsevier: Amsterdam, 1990; p 64.

borrows intensity and polarization through vibronic coupling from the $1B_u$ state. It is possible that the postulated weakly allowed $\sigma\pi^*$ state of Si_6Me_{14} acts similarly and borrows intensity from the strongly allowed $\sigma\sigma^*$ state. Its fluorescence should intrinsically have a negative degree of polarization. The observed positive polarization would have to be borrowed from the σ–σ^* transition along with the intensity.

Temperature Dependence. As shown in Figure 3, the fluorescence quantum yields and lifetimes of Si_6Me_{14} depend on temperature very strongly. The temperature dependence of Φ_F alone might be attributable to the presence of more stable emissive conformers, dominant at low temperatures, and less stable nonemissive ones, dominant at room temperature, although this looks very unlikely because of the enormous decrease of Φ_F at higher temperatures. However, the parallel change in τ_F demonstrates that we are dealing with a rate process. We propose that the rapid decrease of Φ_F and τ_F with increasing temperature is due to the existence of a thermally activated dark channel for the depopulation of the emitting state, competing with fluorescence and characterized by a unimolecular rate constant $k_1(T) = A \exp(-\Delta E/RT)$.

The situation is complicated by the presence of a large number of conformers, each with its own photophysical characteristics, and by the temperature dependence of the conformational equilibrium, suggested by the absorption spectra. The observation that the fluorescence spectrum is nearly independent of temperature and independent of excitation energy, and also the coincidence of the absorption and excitation spectra, limit the possibilities. Either all the conformers have the same photophysical properties or they are all rapidly adiabatically converted upon excitation to a few that do, or perhaps to a single one, with similar losses due to nonradiative processes such as intersystem crossing. We cannot distinguish between these possibilities, and although in the following discussion we refer to the emitting Si_6Me_{14} as a single species, it could well be a mixture of conformers of very similar properties.

The fact that the Φ_F value at 77 K, 0.45, is still far from unity, suggests very strongly that there is also a temperature-independent nonradiative decay pathway for the emitting singlet state, characterized by a unimolecular rate constant k_2. This is likely to be intersystem crossing, but it could also be internal conversion.

The fluorescence quantum yield Φ_F of Si_6Me_{14} can then be written as

$$\Phi_F(T) = k_F/[k_F + k_1(T) + k_2] \quad (2)$$

The observed Φ_F and τ_F values change with temperature in a similar fashion (Figure 3), and $k_F = \Phi_F/\tau_F$ is independent of temperature. The most reliable value of k_F was obtained at 77 K, where the emission is the strongest, and is 3.5×10^8 s^{-1}.

If we now assume that $k_1(T)$ is negligible at 77 K, the rate constant $k_1(T)$ can be calculated from the fluorescence quantum yield

$$k_1(T) = k_F[1/\Phi_F(T) - 1] - k_2 \quad (3)$$

or from the fluorescence lifetime

$$k_1(T) = 1/\tau_F(T) - k_F - k_2 \quad (4)$$

For the rate constant of the temperature-independent dark path,

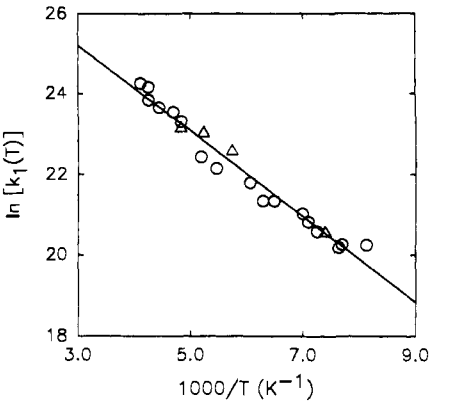

Figure 6. Plot of ln $[k_1(T)]$ against $1/T$ (slope = −1.06, intercept = 28.34, and γ = 0.986).

$k_2 = [1 - \Phi_F(77)]/\tau_F(77) = 4.2 \times 10^8$ s^{-1}, where $\Phi_F(77)$ and $\tau_F(77)$ are the fluorescence quantum yield and lifetime at 77 K, respectively. The plot of ln $[k_1(T)]$ against $1/T$ is close to linear (Figure 6), and its slope yields a barrier height ΔE of 2.1 kcal/mol. The preexponential factor A of 2×10^{12} s^{-1} can be obtained from the intercept and is of unexceptional magnitude for an intramolecular distortion process. If $k_1(T)$ is not yet negligible at 77 K, i.e., if the limiting value of Φ_F is larger than the 0.45 assumed here, the resulting ΔE and A values change somewhat. At the assumed limiting Φ_F value of unity, for which the Arrhenius plot becomes a little curved, one obtains ΔE = 1.8 kcal/mol and $A = 1 \times 10^{12}$ s^{-1}.

At the moment, we have no indication of the detailed nature of the reaction path that takes the already distorted excited molecule to and over this small barrier in its energy surface. It apparently leads to a region of geometries for which radiationless return to the ground state is very fast. It is not clear at this time whether this return leads to a net chemical change or is of photophysical nature.

Conclusions. While the absorption properties of Si_6Me_{14} extrapolate smoothly from those of the longer oligosilane and polysilane chains, its fluorescence properties do not. We propose that the nature of the lowest singlet state changes between $Si_{10}Me_{22}$ and Si_6Me_{14} and favor one of three possible tentative assignments for the emitting state of the latter. The strong temperature dependence of the fluorescence quantum yield has been attributed to the existence of a thermally activated radiationless deactivation process, presumably an escape from the fluorescent minimum over a small barrier (E_a = 2.1 kcal/mol, $A = 2 \times 10^{12}$ s^{-1}).

Acknowledgment. This research was supported by the U.S. Air Force Office of Scientific Research (91-0032). We thank Mr. Thomas H. F. Kammel and Ms. Andrienne C. Friedli for the preparation of permethylhexasilane and Dr. Stephen J. Atherton for his help in the fluorescence lifetime measurement at the Center for Fast Kinetic Research, jointly supported by the Biotechnology Branch of the Division of Research Resources of the National Institute of Health (RR00886) and the University of Texas at Austin.